NUCLEAR THEORY, Vol. 30 (2011)
eds. A. Georgieva, N. Minkov, Heron Press, Sofia

Energies and Transition Probabilities in Nuclear Alternating-Parity Spectra

N. Minkov[1], **S. Drenska**[1], **M. Strecker**[2], **W. Scheid**[2]

[1]Institute of Nuclear Research and Nuclear Energy, Bulgarian Academy of Sciences, Tzarigrad Road 72, BG-1784 Sofia, Bulgaria

[2]Institut für Theoretische Physik der Justus-Liebig-Universität, Heinrich-Buff-Ring 16, D–35392 Giessen, Germany

Abstract.

An extension of the model of Coherent Quadrupole-Octupole Motion (CQOM) is presented which describes energies and transition rates in the yrast and non-yrast alternating-parity spectra of even-even nuclei. Generalized electric transition operators reflecting the complex shape properties associated with the quadrupole-octupole vibration modes are introduced. Model expressions for the B(E1), B(E2) and B(E3) reduced transition probabilities within and between the different energy sequences are derived. It is shown that the model successfully reproduces the yrast and non-yrast alternating-parity levels together with the related B(E1)-B(E3) transition rates in the nuclei ^{152}Sm, ^{154}Gd and ^{236}U.

1 Introduction

The appearance of alternating-parity bands in even-even atomic nuclei, as a result of the presence of quadrupole-octupole deformations, is usually attended by enhanced electric E1 and E3 transitions between levels with opposite parity [1]. The B(E1) and B(E3) reduced transition probabilities are known to provide a sensitive test for the structure of the alternating-parity sequences. Therefore, their description together with the energy levels is of special importance for the explanation of the complex quadrupole-octupole motions of nuclei.

The purpose of the present work is to implement a consistent description of energies and transition probabilities in the yrast and non-yrast alternating-parity bands of even-even nuclei within the model of Coherent Quadrupole-Octupole Motion (CQOM) [2]. In the originally proposed model scheme the yrast alternating-parity band is composed as usual by the members of the ground-state band and the lowest negative-parity levels with odd angular momenta [2]. Recently it was suggested that the model scheme can be extended by assuming that the excited β-bands are connected to higher negative-parity sequences with odd angular momenta [3]. It was shown that the extended CQOM scheme is capable to reproduce the yrast and non-yrast alternating parity levels in rare-earth and actinide nuclei. In the present work the model scheme is further extended to

describe electric transition probabilities by taking into account the properties of the complex quadrupole-octupole motion of the system. The extended model is applied for the simultaneous description of energies and E1, E2 and E3 transition rates in the alternating-parity spectrum.

In Sec. 2 the CQOM model and its extended formalism for the description of B(E1)-B(E3) transition probabilities are shown. In Sec. 3 numerical results and discussion on the application of the model to the nuclei ^{152}Sm, ^{154}Gd and ^{236}U are presented. In Sec. 4 concluding remarks are given.

2 Model of Coherent Quadrupole–Octupole Motion

2.1 Hamiltonian and Wave Functions

The general Hamiltonian of the model is [2]

$$H_{qo} = -\frac{\hbar^2}{2B_2}\frac{\partial^2}{\partial\beta_2^2} - \frac{\hbar^2}{2B_3}\frac{\partial^2}{\partial\beta_3^2} + U(\beta_2,\beta_3,I)\,, \tag{1}$$

where β_2 and β_3 are axial quadrupole and octupole variables, respectively, and

$$U(\beta_2,\beta_3,I) = \frac{1}{2}C_2{\beta_2}^2 + \frac{1}{2}C_3{\beta_3}^2 + \frac{X(I)}{d_2\beta_2^2 + d_3\beta_3^2}\,, \tag{2}$$

with $X(I) = [d_0 + I(I+1)]/2$. Here B_2 (B_3), C_2 (C_3) and d_2 (d_3) are quadrupole (octupole) mass, stiffness and inertia parameters, respectively, while d_0 determines the potential core at $I = 0$. Under the assumption of coherent quadrupole-octupole oscillations with a frequency $\omega = \sqrt{C_2/B_2} = \sqrt{C_3/B_3} \equiv \sqrt{C/B}$, and after introducing ellipsoidal coordinates

$$\beta_2 = p\eta\cos\phi, \qquad \beta_3 = q\eta\sin\phi, \tag{3}$$

with $p = \sqrt{d/d_2},\ q = \sqrt{d/d_3}$ and $d = (d_2+d_3)/2$, the collective energy of the system is obtained in the form [2]

$$E_{n,k}(I) = \hbar\omega\left[2n+1+\sqrt{k^2+bX(I)}\right],\ n=0,1,2,...;\ k=1,2,3,..., \tag{4}$$

where $b = 2B/(\hbar^2 d)$. The quadrupole-octupole vibration wave function is

$$\Phi^{\pi}_{nkI}(\eta,\phi) = \psi^I_{nk}(\eta)\varphi^{\pi}_k(\phi), \tag{5}$$

where the "radial" part

$$\psi^I_{n,k}(\eta) = \sqrt{\frac{2c\Gamma(n+1)}{\Gamma(n+2s+1)}}e^{-c\eta^2/2}(c\eta^2)^s L_n^{2s}(c\eta^2) \tag{6}$$

involves generalized Laguerre polynomials in the variable η with $c = \sqrt{BC}/\hbar$ and $s = (1/2)\sqrt{k^2 + bX(I)}$. The "angular" part in the variable ϕ appears with a positive or negative parity as follows

$$\varphi_k^+(\phi) = \sqrt{2/\pi}\cos(k\phi)\,, \qquad k = 1, 3, 5, \ldots\,, \tag{7}$$

$$\varphi_k^-(\phi) = \sqrt{2/\pi}\sin(k\phi)\,, \qquad k = 2, 4, 6, \ldots\,. \tag{8}$$

The total wave function has the form

$$\Psi^{\pi}_{nIM0}(\eta, \phi) = \sqrt{\frac{2I+1}{8\pi^2}} D^I_{M\,0}(\theta)\psi^I_n(\eta)\varphi^{\pm}(\phi)\,. \tag{9}$$

The energy spectrum is determined in (4) by the quantum numbers n and k. An alternating-parity band is determined by given n and a pair of odd and even k-values, $k_n^{(+)}$ and $k_n^{(-)}$, corresponding to the positive and negative parity sequence, respectively. As suggested in [3] the sets of levels labeled by $n = 0, 1$ and 2 involve the ground-state band, first and second β-bands, respectively.

2.2 Transition Probabilities

The B(Eλ) transition probabilities between model states (9) are determined by

$$B(E\lambda; n_i k_i I_i \to n_f k_f I_f) =$$
$$= \frac{1}{2I_i + 1} \sum_{M_i M_f \mu} \left| \left\langle \Psi^{\pi_f}_{n_f k_f I_f M_f 0}(\eta, \phi) \middle| \mathcal{M}_\mu(E\lambda) \middle| \Psi^{\pi_i}_{n_i k_i I_i M_i 0}(\eta, \phi) \right\rangle \right|^2. \tag{10}$$

The operators for electric E1, E2 and E3 transitions are defined as

$$\mathcal{M}_\mu(E\lambda) = \sqrt{\frac{2\lambda+1}{4\pi(4 - 3\delta_{\lambda,1})}} \hat{Q}_{\lambda 0} D^\lambda_{0\mu}, \;\; \lambda = 1, 2, 3, \;\; \mu = 0, \pm 1, ..., \pm\lambda. \tag{11}$$

The vibration parts of these operators can be determined as

$$\hat{Q}_{10} = M_1 \beta_2 \beta_3 = M_1 pq\eta^2 \cos\phi \sin\phi \tag{12}$$

$$\hat{Q}_{20} = M_2 \beta_2 = M_2 p\eta \cos\phi \tag{13}$$

$$\hat{Q}_{30} = M_3 \beta_3 = M_3 q\eta \sin\phi, \tag{14}$$

with $q = p/\sqrt{2p^2 - 1}$. The electric charge factors M_λ are taken as [4]

$$M_\lambda = \frac{3}{\sqrt{(2\lambda+1)\pi}} ZeR_0^\lambda, \qquad \lambda = 2, 3\,, \tag{15}$$

$$M_1 = \frac{9AZe^3}{56\sqrt{35}\pi} \left(\frac{1}{J} + \frac{15}{8QA^{\frac{1}{3}}} \right), \tag{16}$$

where $R_0 = r_0 A^{1/3}$, $r_0 \approx 1.2$ fm, Z is the proton number, and e is the elementary electric charge. Since there is not a unique approach to estimate the factor M_1 in the present work an effective charge $e^1_{\rm eff}$ is used in (16) instead of e. The quantities $J = 35$ MeV and $Q = 45$ MeV are taken with fixed values in all considered nuclei.

The definitions of operators (12)–(14) originally correspond to a situation in which the nuclear shape is characterized by fixed values of the deformation parameters β_2 and β_3. In this case the density distribution of the collective state is characterized by a single maximum in the space of β_2 and β_3. In the case of the model potential (2) taken with an elliptic bottom the density distribution can be characterized by more than one maximum. This is illustrated in Figure 1, where the density distribution $|\Phi^{\pi}_{nkI}(\beta_2,\beta_3)|^2$ of the state (5) is plotted for different k-values at $n = 0$ after transforming to (β_2,β_3) variables.

To describe the transition between the states with different numbers of maxima the angular parts in (12)–(14) are generalized through the replacements

$$\cos\phi \to A_{20}(\phi) = \sum_{k=1}^{\infty} \frac{\cos(k\phi)}{k} = -\frac{1}{2}[\ln 2 + \ln(1-\cos\phi)] \tag{17}$$

$$\sin\phi \to A_{30}(\phi) = \sum_{k=1}^{\infty} \frac{\sin(k\phi)}{k} = \frac{\pi-\phi}{2} + \pi\text{Floor}\left(\frac{\phi}{2\pi}\right) \tag{18}$$

$$\cos\phi\sin\phi \to \hat{A}_{10}(\phi) \equiv \sum_{m=1}^{\infty}\sum_{n=1}^{\infty} \frac{\cos(m\phi)}{m}\frac{\sin(n\phi)}{n}. \tag{19}$$

Here expansion (19) is reasonably convergent. The expressions (17) and (18) represent even and odd Fourier expansion series, respectively. The first terms in (17) and (19) represent the original angular (ϕ-) parts in operators (12)–(14). Now these operators are redefined as

$$\hat{Q}_{10}(\eta,\phi) = M_1 pq\eta^2 A_{10}(\phi) \tag{20}$$

$$\hat{Q}_{20}(\eta,\phi) = M_2 p\eta A_{20}(\phi) \tag{21}$$

$$\hat{Q}_{30}(\eta,\phi) = M_3 q\eta A_{30}(\phi). \tag{22}$$

After carrying out the integration over the rotation part in (10) one obtains

$$B(E\lambda; n_i k_i I_i \to n_f k_f I_f) = \\ = \frac{2\lambda+1}{4\pi(4-3\delta_{\lambda,1})}\langle I_i 0\lambda 0|I_f 0\rangle^2 R^2_\lambda(n_i k_i I_i \to n_f k_f I_f), \tag{23}$$

with

$$R_\lambda(n_i k_i I_i \to n_f k_f I_f) = \left\langle \Phi^{\pi_f}_{n_f k_f I_f}(\eta,\phi)\left|\hat{Q}_{\lambda 0}\right|\Phi^{\pi_i}_{n_i k_i I_i}(\eta,\phi)\right\rangle. \tag{24}$$

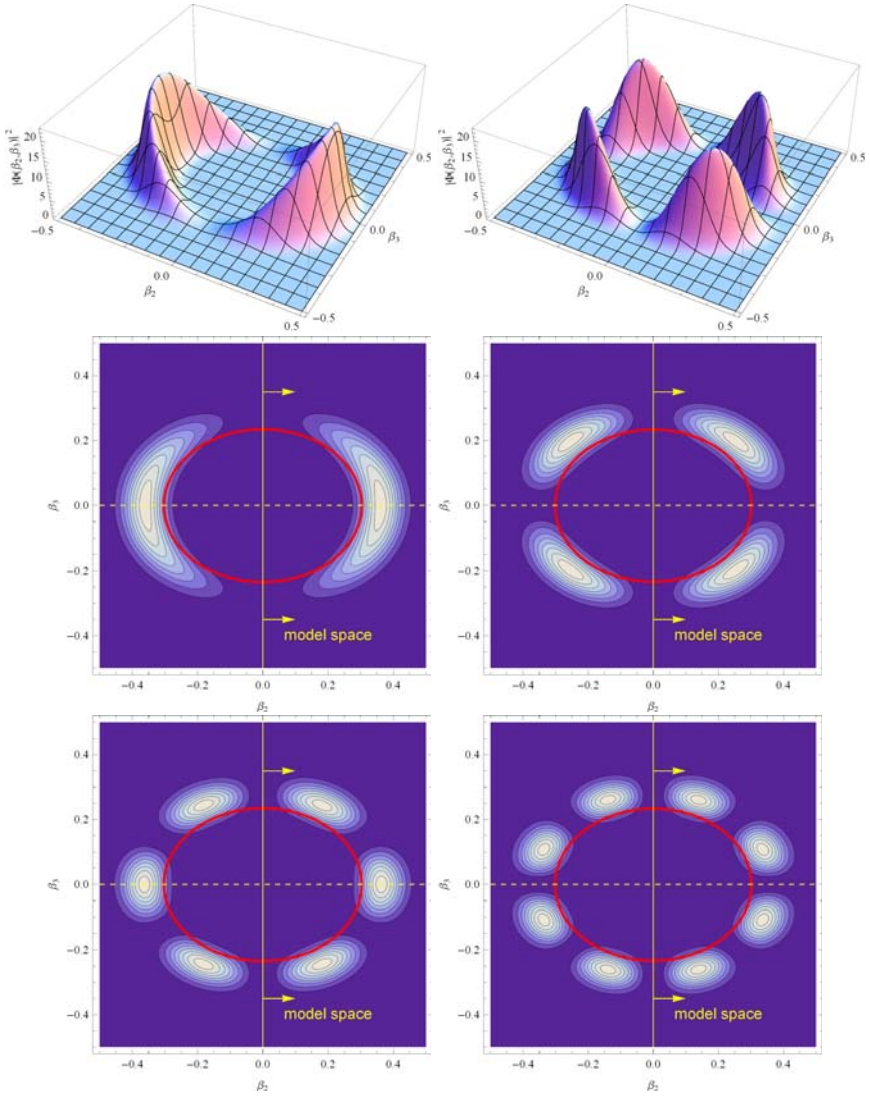

Figure 1. Schematic 3D and 2D contour plots of the density distribution $|\Phi^{\pi}_{nkI}(\beta_2,\beta_3)|^2$ for $k=1$, $I=2$ (up/mid left) and $k=2$, $I=1$ (up/mid right), $k=3$, $I=2$ (down left) and $k=4$, $I=1$ (down right) at $n=0$. The ellipsoidal curves outline the potential bottom. The model space corresponds to the $\beta_2>0$ half-plane.

By further separating the integrations over the "radial" variable η and the "angular" variable ϕ in (24) according to (5) one obtains

$$R_1(n_ik_iI_i \to n_fk_fI_f) = M_1pqS_2(n_i,I_i;n_f,I_f)I_1^{\pi_i,\pi_f}(k_i,k_f) \qquad (25)$$

$$R_2(n_i k_i I_i \to n_f k_f I_f) = M_2 p S_1(n_i, I_i; n_f, I_f) I_2^{\pi_i,\pi_f}(k_i, k_f) \tag{26}$$

$$R_3(n_i k_i I_i \to n_f k_f I_f) = M_3 q S_1(n_i, I_i; n_f, I_f) I_3^{\pi_i,\pi_f}(k_i, k_f), \tag{27}$$

where

$$S_1(n_i, I_i; n_f, I_f) = \int_0^\infty d\eta \psi_{n_f}^{I_f}(\eta)\eta^2\psi_{n_i}^{I_i}(\eta) \tag{28}$$

$$S_2(n_i, I_i; n_f, I_f) = \int_0^\infty d\eta \psi_{n_f}^{I_f}(\eta)\eta^3\psi_{n_i}^{I_i}(\eta), \tag{29}$$

and

$$I_\lambda^{\pi_i,\pi_f}(k_i, k_f) = \frac{2}{\pi}\int_{-\frac{\pi}{2}}^{\frac{\pi}{2}} A_{\lambda 0}(\phi)\varphi_{k_f}^{\pi_f}(\phi)\varphi_{k_i}^{\pi_i}(\phi)d\phi, \quad \lambda = 1, 2, 3. \tag{30}$$

The integrals over η, (28) and (29), involve the "radial" wave functions (6) and can be expressed in the following analytic form

$$\begin{aligned} S_l(n_i, I_i; n_f, I_f) = {} & \frac{1}{c^{l/2}}\Big[\frac{\Gamma(n_f+1)\Gamma(n_i+1)}{\Gamma(n_f+2s_f+1)\Gamma(n_i+2s_i+1)}\Big]^{\frac{1}{2}} \\ & \times \frac{\Gamma(n_f+2s_f+1)}{\Gamma(1+2s_f)}\frac{\Gamma(n_i+s_i-s_f-l/2)}{\Gamma(s_i-s_f-1)}\frac{\Gamma(s_i+s_f+l/2+1)}{n_i!n_f!} \\ & \times {}_3F_2(-n_f, s_i+s_f+\frac{l}{2}+1, s_f-s_i+\frac{l}{2}+1; 2s_f+1, s_f-s_i+\frac{l}{2}+1-n_i; 1), \\ & l = 1, 2, \end{aligned} \tag{31}$$

where ${}_3F_2$ denotes the generalized hypergeometric function [5]. The integrals over ϕ (30) involve the "angular" wave functions (7) and (8) and also can be expressed in explicit forms by using integration of products of trigonometric functions.

3 Numerical Results and Discussion

The extended CQOM formalism is applied to the nuclei ^{152}Sm, ^{154}Gd and ^{236}U. The model energy levels are determined by Eq. (4) as $\tilde{E}_{n,k}(I) = E_{n,k}(I) - E_{0,k_0^{(+)}}(0)$. The parameters ω, b, d_0, c, p and e^1_{eff} are adjusted by simultaneously taking into account experimental data on the energy bands [6] and the available B(E1)-B(E3) transition probabilities [7], [8]. For each nucleus the calculations are performed in a net over the values of $k_n^{(+)}$ and $k_n^{(-)}$ providing the sets of k-values for the best description. The theoretical and experimental energy levels and transition probabilities for the three nuclei are compared in Figures 2–4. The obtained parameter values and k-numbers are also given there. It is seen that the model correctly reproduces the structure of the yrast and non-yrast alternating-parity bands. Note that in ^{154}Gd three alternating-parity bands are described in

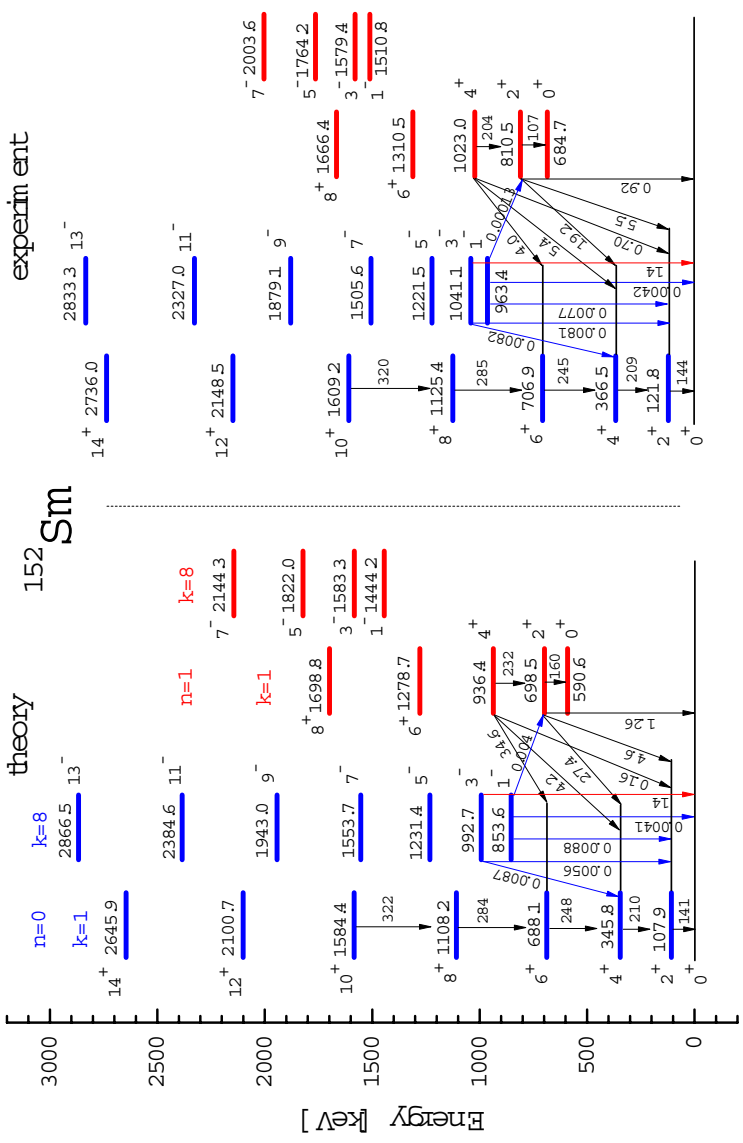

Figure 2. Theoretical and experimental alternating parity levels and transition probabilities for ^{152}Sm. Data for energy levels from [6]. B(E1) and B(E2) data from [7] and B(E3) data from [8]. Parameter values: $\omega = 0.295$ MeV/$\hbar$, $b = 2.450\ \hbar^{-2}$, $d_0 = 78.8\ \hbar^2$, $c = 113.2$, $p = 0.854$, $e^1_{\rm eff} = 1.01\ e$.

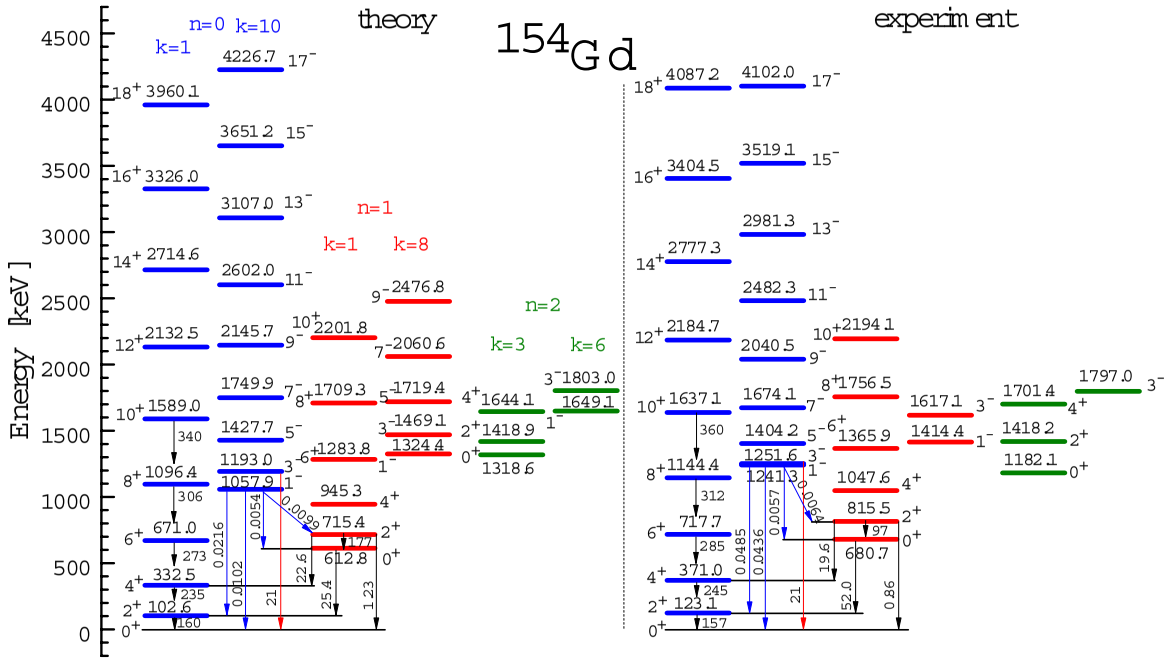

Figure 3. Theoretical and experimental alternating-parity levels and transition probabilities for ^{154}Gd. Data for energy levels from [6]. B(E1) and B(E2) data from [7] and B(E3) data from [8]. Parameter values: $\omega = 0.306$ MeV/$\hbar$, $b = 2.948\ \hbar^{-2}$, $d_0 = 114.7\ \hbar^2$, $c = 113.4$, $p = 0.777$, $e^1_{\rm eff} = 1.048\ e$.

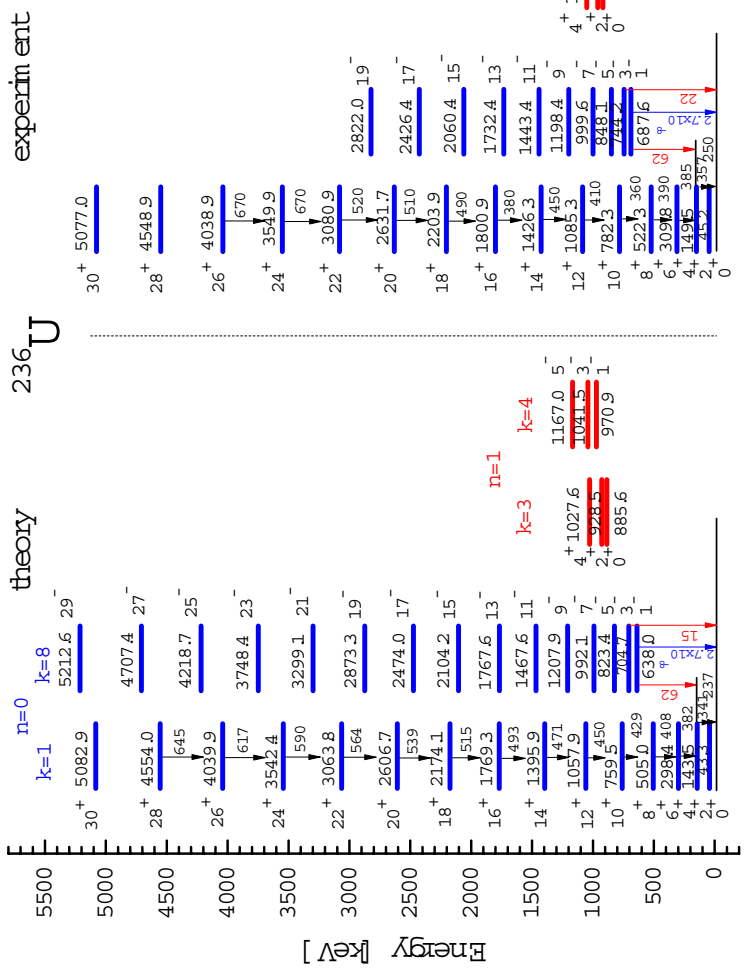

Figure 4. Theoretical and experimental alternating parity levels and transition probabilities for ^{236}U. Data for energy levels from [6]. B(E1) and B(E2) data from [7] and B(E3) data from [8]. $\omega = 0.402$ MeV/$\hbar$, $b = 1.404\ \hbar^{-2}$, $d_0 = 539.3\ \hbar^2$, $c = 343.4$, $p = 0.949$, $e^1_{\rm eff} = 0.134\ e$.

total. In the three nuclei the B(E1) transition probabilities between the ground-state band (gsb) and the first negative-parity band are described quite well. The value of the interband B(E1) probability B(E1;$1^-_1 \rightarrow 2^+_2$) in ^{152}Sm is overestimated by one order while the B(E1;$1^-_1 \rightarrow 0^+_2$) and B(E1;$1^-_1 \rightarrow 2^+_2$) values in ^{154}Gd are well described. The B(E2) intraband probabilities within the gsb of ^{152}Sm and ^{154}Gd are well described, while in ^{236}U the description is good as overall up to a quite high $I = 26$. The E2 interband transitions between members of the first β-band and gsb in ^{152}Sm and ^{154}Gd are also well described with a few exceptions. The B(E3;$3^-_1 \rightarrow 0^+_1$) values in ^{152}Sm and ^{154}Gd are exactly reproduced. In ^{236}U this probability is a bit underestimated but, the B(E3;$1^-_1 \rightarrow 4^+_1$) value is exactly reproduced.

4 Conclusion

In conclusion, the present work provides an extended scheme of the collective model of Coherent Quadrupole and Octupole Motion (CQOM) capable of describing the yrast and non-yrast alternating parity spectra and the attendant B(E1), B(E2) and B(E3) transition probabilities in even-even nuclei. The theoretical formalism and the obtained model descriptions for the nuclei ^{152}Sm, ^{154}Gd and ^{236}U outline a possible way for the development of nuclear alternating-parity spectra towards the highly non-yrast region of collective excitations. The results suggest that a similar extension of the model can be reasonable for the non-yrast spectra of odd-mass nuclei with quadrupole-octupole deformations. This is the subject of further work.

Acknowledgements

This work is supported by DFG and by the Bulgarian National Science Fund (contract DID-02/16-17.12.2009).

References

[1] P.A. Butler and W. Nazarewicz, *Rev. Mod. Phys.* **68** (1996) 349.

[2] N. Minkov, P. Yotov, S. Drenska, W. Scheid, D. Bonatsos, D. Lenis and D. Petrellis, *Phys. Rev. C* **73** (2006) 044315.

[3] N. Minkov, S. Drenska and W. Scheid, In: *Nuclear Theory*, vol. **29**, *Proceedings of the 29-th International Workshop on Nuclear Theory (Rila, Bulgaria 2010)*, edited by A.I. Georgieva and N. Minkov, Heron Press, Sofia (2010) 189.

[4] V.Yu. Denisov and A.Ya. Dzyublik, Nucl. Phys. A **589** (1995) 17.

[5] L.J. Slater, *Generalized Hypergeometric Functions*, Cambridge University Press, Cambridge (1987); http://mathworld.wolfram.com/GeneralizedHypergeometricFunction.html

[6] http://www.nndc.bnl.gov/ensdf/. Data as of August 2011.

[7] http://www.nndc.bnl.gov/nudat2/indx_adopted.jsp. Data as of August 2011.

[8] T. Kibedi and R.H. Spear, At. Data Nucl. Data Tables **80** (2002) 35-82.